Optical control of light propagation in photonic crystal based on electromagnetically induced transparency*

Dan Wang(王丹)[1,2], Jin-Ze Wu(武晋泽)[1,2], and Jun-Xiang Zhang (张俊香)[1,2,†]

[1] The State Key Laboratory of Quantum Optics and Quantum Optics Devices, Institute of Opto-Electronics, Shanxi University, Taiyuan 030006, China
[2] Collaborative Innovation Center of Extreme Optics, Shanxi University, Taiyuan 030006, China

(Received 3 February 2016; revised manuscript received 15 March 2016; published online 25 May 2016)

A kind of photonic crystal structure with modulation of the refractive index is investigated both experimentally and theoretically for exploiting electromagnetically induced transparency (EIT). The combination of EIT with periodically modulated refractive index medium gives rise to high efficiency reflection as well as forbidden transmission in a three-level atomic system coupled by standing wave. We show an accurate theoretical simulation via transfer-matrix theory, automatically accounting for multilayer reflections, thus fully demonstrate the existence of photonic crystal structure in atomic vapor.

Keywords: electromagnetically induced transparency, periodical refractive index modulation, transfer-matrix method, Bragg reflection

PACS: 42.50.Gy, 42.70.Qs, 42.30.Rx **DOI:** 10.1088/1674-1056/25/6/064202

1. Introduction

Electromagnetically induced transparency[1,2] (EIT) is a fascinating quantum coherence phenomenon to suppress resonant absorption[3] and slow light pulse,[4] manipulate atomic entanglement,[5] and realize high efficiency quantum memory.[6,7] It has been successfully integrated on a semiconductor chips,[8] promoting the development of quantum optical device. Recently, EIT shows the wide applications in the field of cavity optomechanics,[9] optical lattice for cold atoms,[10] and hybrid atom-molecular system.[11,12] Photonic crystal structure[13–16] with periodically varying refractive index is capable of controlling the flow of light wave. The main feature is to open photonic band gaps (PBGs) resulting from Bragg scattering.

The combination of EIT and photonic crystal is an attractive research for quantum communication network. EIT-based photonic crystal structure can be constructed in a three-level atomic system driven by a standing wave, which results in spatially modulated absorption and refractive index.[17] This photonic crystal structure generates a reflected field, which is explained as either electromagnetically induced grating (EIG)[18–20] or four-wave mixing (FWM) process.[21,22] At the same time of reflection, electromagnetically induced absorption (EIA)[23] happened to the probe field in thermal vapor. Therefore, much attention has been paid to the applications in all-optical routing,[24] optical controllable Bragg mirror,[25] and optical diode.[26] Bae *et al.* and Andy *et al.* observed reflection signals with efficiencies of 11.5%[20] and 7%,[24] respectively, accompanying a decrease in transmittance of the probe field[19,20,24] due to EIG reflections and spatial interference effects from the modulated absorption in rubidium atoms. For the application in high performance quantum optical device, we should improve the reflection efficiency to a higher level as well as achieve strong absorption. Here, we experimentally obtain 35% reflection and simultaneously achieve the complete opaque to the probe field in a spatially modulated photonic crystal grating with cesium vapor.

In these previous studies, diffraction/reflection signals were obtained by solving the wave equation of the probe field with the consideration of spatial modulation of coupling field.[18] On the other side, the explanation of FWM[21,22] focused on the nonlinear susceptibility exploiting perturbation theory without regard to the spatial modulation. In the present paper, by combing the periodic modulation and EIT, we show good agreement between numerical simulation and experimental observation with using the transfer-matrix theory,[27,28] which is proved to be the most effective method to study the light propagation in periodically modulated dielectric. The consistence fully demonstrates the existence of periodic modulation thereby helpfully understanding the physics behind multilayer reflections in photonic crystal structure.

2. Experiment

We perform the experiment in a three-level system with one excited level $|a\rangle$ $(6^2P_{1/2}, F' = 4)$, and two ground levels $|b\rangle$ $(6^2S_{1/2}, F = 4)$ and $|c\rangle$ $(6^2S_{1/2}, F = 3)$ of the ^{133}Cs D1 line, see Fig. 1(a). The resonant transition frequencies

*Project supported by the National Natural Science Foundation of China (Grant No. 11574188) and the Project for Excellent Research Team of the National Natural Science Foundation of China (Grant No. 61121064).

†Corresponding author. E-mail: junxiang@sxu.edu.cn

of $|a\rangle \leftrightarrow |b\rangle$ and $|a\rangle \leftrightarrow |c\rangle$ are denoted as ω_{ab} and ω_{ac}, respectively. Spontaneous decay rate of the excited level is $\Gamma = 2\pi \times 4.6$ MHz. Two counter-propagating horizontally linearly polarized coupling fields with equal frequency $\omega_c = \omega_{ac}$ propagate along the x direction. A vertically linearly polarized probe field ω_p is frequency scanned in the vicinity of $|a\rangle \leftrightarrow |b\rangle$ with detuning $\Delta_p = \omega_p - \omega_{ab}$ and enters into the vapor cell at an angle of $\theta = 0.14^\circ$ with respect to the coupling field. In experiment, we control the atom temperature at $T = 60$ °C. The powers of the counter-propagating coupling fields are both 20 mW with e^{-2} full width of 0.64 mm, and the power of the probe field is 50 μW with e^{-2} full width of 0.59 mm. The probe intensity is detected by PD1, and the reflective field (blue dashed line) is collected by PD2 in the reverse direction.

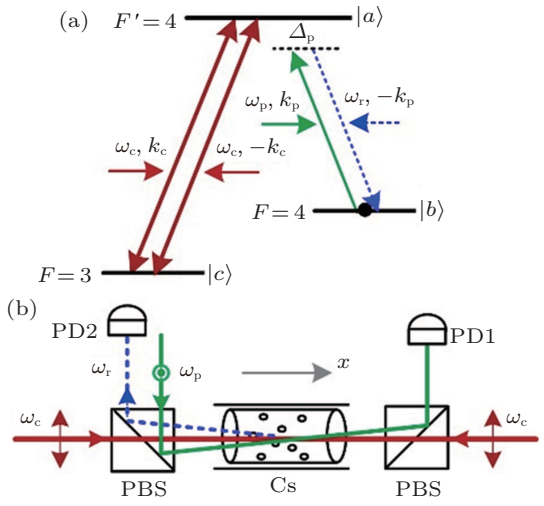

Fig. 1. (color online) (a) Λ-type three-level system driven by standing wave (SW) coupling field. (b) Experimental setup. PBS: polarizing beam splitters, PD: photo detector.

If the backward coupling field is blocked, this atom-field interaction exhibits typical EIT as shown in Fig. 2(a). There is no reflection signal to be detected by PD2, at the same time, the probe field propagates with transmission $T = 80\%$ at resonant frequency ($T = P_{out}/P_{in}$, P_{out} and P_{in} are the powers of the output and input probe fields). When the backward coupling field is switched on, an SW is formed with intensity modulation at half wavelength. Then, the probe absorption is periodically modulated as a grating. This grating structure results in the reflection signal of probe field with efficiency $R = 35\%$ ($R = P_r/P_{in}$, P_r is the power of the reflected field), see the red curve in Fig. 2(b). The generation of reflection signal can be explained as either FWM[21,22] or Bragg scattering[18–20,24] originating from the periodicity of refractive index. We will focus on the latter explanation in the following. The accompanying transmission at one- and two-photon resonance $\Delta_p = 0$ is transformed from EIT into forbidden transmission, see the black curve in Fig. 2(b). This forbidden transmission is the result of velocity selective effect. For thermal atoms moving with nonzero velocity along the x direction, the frequencies of the counter-propagating coupling fields are different from each other due to Doppler Effect. Therefore, the on-resonance enhanced absorption is attributed to the interaction with slow atoms, and two transparency windows around the resonant point are EIT contributed by two groups of atoms with opposite velocities. In a word, high-efficiency reflection as well as completely opacity is consistent with the effect of photonic band gap, and it is promising to be applied as a quantum optical device.

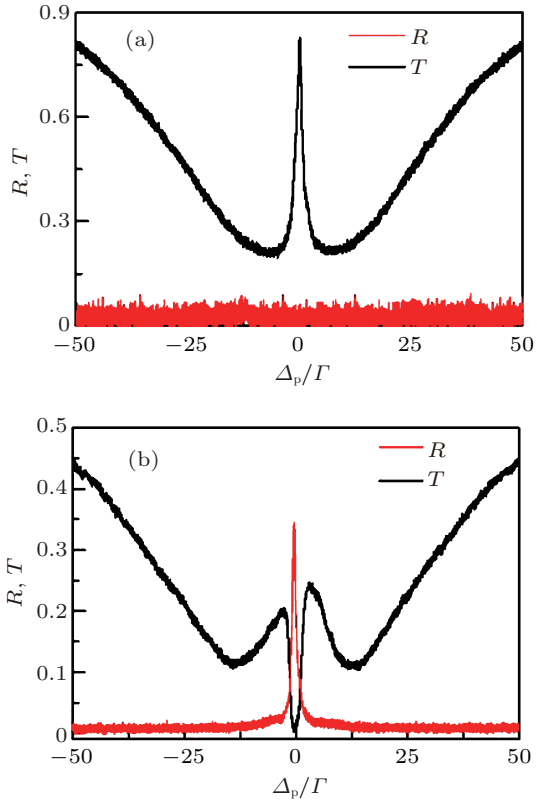

Fig. 2. (color online) The probe reflection (red curve) and transmission (black curve) spectra. (a) Typical EIT when the backward coupling field is absent. (b) The atomic system is coupled by SW.

3. Theoretical calculation

SW coupling field varies the absorption of probe field along the x direction with a periodicity of $a = \lambda_c/2$. Then, the periodical modulation of absorption gives rise to a similar modulation of refractive index limited by Kramers-Kronig relations[29] as shown in Fig. 3. The probe field "sees" the atomic vapor like a one-dimensional (1D) array of thin atomic slabs with periodicity a.

3.1. Periodic modulation of the refractive index

Considering the optical transition of $|a\rangle \leftrightarrow |b\rangle$ driven by the weak probe field, off-diagonal density matrix element ρ_{ab} is represented as a Fourier series in this periodical modulated dielectric

$$\rho_{ab} = e^{ik_p x} \sum_{n=-\infty}^{\infty} \tilde{\rho}_{ab}^{[n]} e^{-2nik_c x}, \quad (1)$$

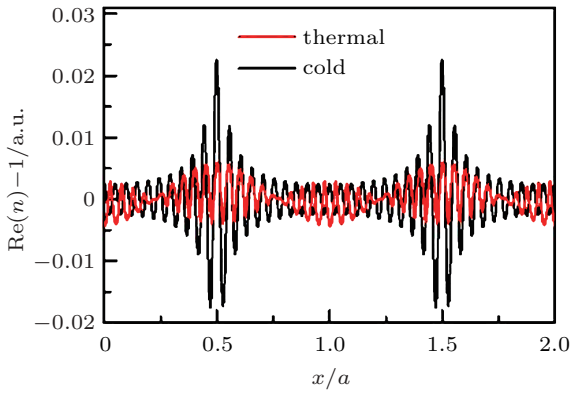

Fig. 3. (color online) Periodic refractive index pattern. Red curve (multiplied by a factor of 100) is for the thermal atoms with $N_0 = 10^{16}$ m^{-3}, black curve is for the ultracold atoms with $N_0 = 10^{18}$ m^{-3}. Other parameters are $\Omega_{c1} = \Omega_{c2} = 5\Gamma$, $\Delta_p = 0.05\Gamma$, and $\lambda_c = 894.576$ nm.

which is the superposition of infinite spatial harmonics. In Eq. (1), k_p and k_c are the vacuum wavenumbers of the probe and coupling fields respectively. The Rabi frequencies of the probe, forward and backward coupling fields are denoted as Ω_p, Ω_{c1}, and Ω_{c2}, respectively. Fourier coefficients $\tilde{\rho}_{ab}^{[n]}$ are solved by the method of continued fractions.[21,22]

For an atom moving with velocity v along the x direction, the frequencies of the probe, forward and backward coupling fields are Doppler shifted by $k_p v$, $k_c v$, and $-k_c v$, respectively. Consequently, the two counter-propagating coupling fields have a frequency difference $2k_c v$. The optical responses for all atoms with Maxwell velocity distribution $f(v) = \exp\left(-v^2/u^2\right)/u\sqrt{\pi}$ are calculated by integrating Eq. (1) with

$$\chi\left(\Delta_p, x\right) = \frac{3\pi N_0 \gamma_{ab}}{\Omega_p}\left(\frac{\lambda_0}{2\pi}\right)^3 \times \int_{-\infty}^{\infty} \rho_{ab}\left(\Delta_p - k_p v, x\right) f(v)\,\mathrm{d}v, \tag{2}$$

where $u = \sqrt{2k_B T/m_a}$ is the most probable velocity of atoms at a given temperature T, m_a is the atomic mass, and k_B is the Boltzmann constant $\lambda_0 = 894.6$ nm and $\gamma_{ab} = 0.5\Gamma$ are the resonant wavelength and decoherence rate of transition $|a\rangle \leftrightarrow |b\rangle$, respectively and N_0 is the atomic number density. Thus, complex refractive index $n\left(\Delta_p, x\right) = \sqrt{1 + \chi\left(\Delta_p, x\right)}$.

It can have a good accuracy to sum the spatial harmonics from $n = -20$ to 20 in Eq. (1). Consequently, $\mathrm{Re}[n(x)] - 1$ exhibits a spatial modulated wave packet with periodicity a as shown in Fig. 3. Compared with ultracold atoms, blurry spatial modulation of refractive index is shown in thermal atoms because of Doppler shift and smaller atomic density.

3.2. Probe reflection and transmission

Transfer matrix relates forward- and backward-going waves on both sides of an arbitrary optical element.[27] In order to describe the probe propagation through multilayer dielectric, the field amplitude at arbitrary position x is divided into both forward- and backward-going parts as shown in Fig. 4, and regarded as the two elements of a two-dimensional (2D) column vector.

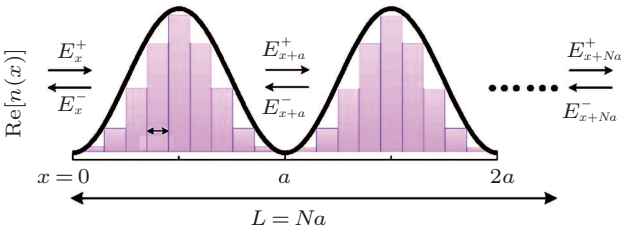

Fig. 4. (color online) Illustration of transfer-matrix method in a periodical modulated 1D atomic array.

As shown in Fig. 3, the photonic crystal structure is not an array of homogeneous thin atom layers but an array of inhomogeneous thin atom layers with a function of $n\left(\Delta_p, x\right)$ in each period. To obtain more accurate numerical simulation, we divide single period into l small slices with each slice occupying an identical thickness of a/l, sufficiently smaller than a. The more slices is divided, the more accurate simulation will be obtained, see Fig. 4. The probe field amplitude experiencing a single period is expressed by

$$\begin{pmatrix} E_{x+a}^+ \\ E_{x+a}^- \end{pmatrix} = M \begin{pmatrix} E_x^+ \\ E_x^- \end{pmatrix} = \prod_{j=l}^{1} m_j \begin{pmatrix} E_x^+ \\ E_x^- \end{pmatrix}, \tag{3}$$

where E^+ and E^- are the forward and backward-going parts at arbitrary position, respectively, M is the primitive cell transfer matrix, and m_j is the transfer matrix of the j-th slice in one cell[27] with

$$m_j = \frac{1}{4n}\begin{pmatrix} (n+1)^2 \mathrm{e}^{\mathrm{i}nk_p a/l} - (n-1)^2 \mathrm{e}^{-\mathrm{i}nk_p a/l} & \left(n^2-1\right)\mathrm{e}^{\mathrm{i}nk_p a/l} - \left(n^2-1\right)\mathrm{e}^{-\mathrm{i}nk_p a/l} \\ \left(n^2-1\right)\mathrm{e}^{-\mathrm{i}nk_p a/l} - \left(n^2-1\right)\mathrm{e}^{\mathrm{i}nk_p a/l} & (n+1)^2 \mathrm{e}^{-\mathrm{i}nk_p a/l} - (n-1)^2 \mathrm{e}^{\mathrm{i}nk_p a/l} \end{pmatrix}, \tag{4}$$

with $\det m_j = 1$ and $\det M = 1$. For simplicity, we denote $n\left[\Delta_p, x + (j-1)a/l\right]$ as n.

The grating period is $a = \lambda_c/2 \approx 447$ nm, therefore, 75-mm-long atomic vapor can be regarded as the stack of an abundance of but finite periods in experiment, whose length is $L = Na$ ($N \gg 1$ is the number of periods). The probe amplitude at the exit of the cell is expressed by

$$\begin{pmatrix} E_{x+Na}^+ \\ E_{x+Na}^- \end{pmatrix} = M_N \begin{pmatrix} E_x^+ \\ E_x^- \end{pmatrix}, \tag{5}$$

where $M_N = M^N = u_{N-1}(\alpha) M - u_{N-2}(\alpha) I$, with I being a

2×2 identity matrix,

$$u_N(\alpha) = \sin\left[(N+1)\cos^{-1}\alpha\right]/\left(1-\alpha^2\right)^{1/2},$$

and $\alpha = \mathrm{Tr}M/2$.[27]

In addition, transfer matrix M_N holds the expression of

$$M_N = \frac{1}{T_N}\begin{pmatrix} T_N^2 - R_N^2 & R_N \\ -R_N & 1 \end{pmatrix}, \tag{6}$$

where R_N and T_N are the amplitude reflectivity and transmittivity of the incident probe field respectively. Finally, one obtains

$$R_N = \frac{M_{12}\sin N\kappa a}{M_{22}\sin N\kappa a - \sin(N-1)\kappa a}, \tag{7}$$

$$T_N = \frac{\sin \kappa a}{M_{22}\sin N\kappa a - \sin(N-1)\kappa a}, \tag{8}$$

where M_{12} and M_{22} are the elements of M. Then, we can directly study the probe reflection $R = |R_N|^2$ and transmission $T = |T_N|^2$ spectra.

3.3. Numerical simulation

Figure 5(a) shows a very accurate numerical simulation of probe reflection and transmission spectra with taking into account the periodic modulation of refractive index. The consistence between theory and experiment demonstrates that the efficient on-resonance Bragg reflection signal and strong absorption are both induced by photonic crystal structure based on EIT. Near-resonant expanded view for Fig. 5(a), which is shown in Fig. 5(b), shows that the sign of photonic stop band gap occurs in thermal vapor. The location of this PBG is limited by Bragg condition $\lambda_0 = n(\Delta_p)\lambda_c\cos\theta$. Therefore, the gap position is optically tunable by controlling the wavelength of coupling field and angle between coupling and probe fields. Referring to result shown in Fig. 3, large spatial modulation of refractive index in ultracold atoms is probable to open a perfect band gap. Therefore, we plot the probe reflection and transmission in Fig. 5(c). Perfect PBG occurs in the frequency region of $\Delta_p \in [0, 0.16\Gamma]$ with nearly 100% reflection and zero transmission.

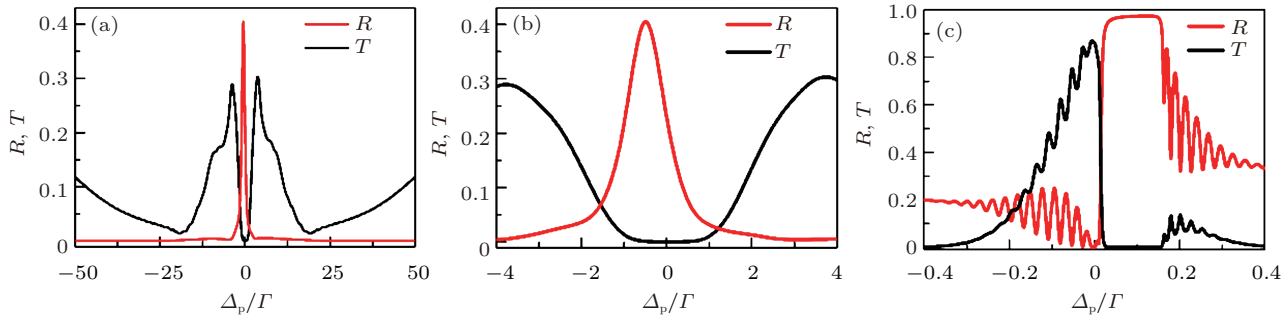

Fig. 5. (color online) Theoretical simulations of probe reflection (red curve) and transmission spectra (black curve). Panels (a) and (b) are for Doppler-broaden thermal atoms with $u = 250$ m/s, panel (b) is for the near-resonant expanded view in panel (a), the other parameters are the same as those in Fig. 3. Panel (c) is for the ultracold atoms driven by non-perfect SW with $\Omega_{c2}/\Omega_{c1} = 0.8$. In numerical calculation, a single period is divided into $l = 50$ slices and the number of periods is set to be $N = 1.6\times10^5$.

4. Conclusion and perspectives

In this work, we experimentally investigate a kind of photonic crystal structure in three-level cesium vapor driven by standing wave coupling field. A similar effect of frequency stop band, on-resonance high-efficiency Bragg reflection signal and forbidden transmission are obtained. Transfer-matrix method is used to give a very good numerical simulation with taking into account the characteristic of periodic refractive index modulation. It is proved that photonic crystal structure really exists in this coupled atom-field system due to the consistence between experimental and theoretical results. Furthermore, perfect PBG is predicted in ultracold atoms, providing potential applications in optical communication network and promise to be integrated on chip.

Acknowledgment

We would like to thank Shangqi Kuang for helpful discussion.

References

[1] Harris S E 1997 *Phys. Today* **50** 36
[2] Wang M, Bai J H, Pei L Y, Lu X G, Gao Y L, Wang R Q, Wu L A, Yang S P, Pang Z G, Fu P M and Zuo Z C 2015 *Acta Phys. Sin.* **64** 0154208 (in Chinese)
[3] Xiao M, Li Y Q and Jin S Z 1995 *Phys. Rev. Lett.* **74** 666
[4] Hau L V, Harris S E, Dutton Z and Behroozi C H 1999 *Nature* **397** 594
[5] Jing H, Liu X J, Ge M L and Zhan M S 2005 *Phys. Rev. A* **71** 062336
[6] Fleischhauer M and Lukin M D 2002 *Phys. Rev. A* **65** 022314
[7] Julsgaard B, Sherson J, Cirac J I, Fiurášek J and Polzik E S 2004 *Nature* **432** 482
[8] Schmidt H and Hawkins A R 2005 *Appl. Phys. Lett.* **86** 032106
[9] Jing H, Özdemir S K, Geng Z, Zhang J, Lü X Y, Peng B, Yang L and Nori F 2015 *Sci. Rep.* **5** 9663
[10] Schnorrberger U, Thompson J D, Trotzky S, Pugatch R, Davidson N, Kuhr S and Bloch I 2009 *Phys. Rev. Lett.* **103** 033003
[11] Jing H, Deng Y G and Zhang W P 2009 *Phys. Rev. A* **80** 025601
[12] Jing H, Deng Y G and Meystre P 2011 *Phys. Rev. A* **83** 063605
[13] Sakoda K. 2001 Optical properties of photonic crystals (Berlin: Springer), p. 2
[14] Chen S, Xie S Y, Yang Y P and Chen H 2003 *Acta Phys. Sin.* **52** 0853 (in Chinese)
[15] Xing R, Xie S Y, Xu J P and Yang Y P 2014 *Acta Phys. Sin.* **63** 094205 (in Chinese)
[16] Fan C Z, Wang J Q, He J N, Ding P and Liang E J 2013 *Chin. Phys. B* **22** 074211

[17] Bajcsy M, Zibrov A S and Lukin M D 2003 *Nature* **426** 638
[18] Ling H Y, Li Y Q and Xiao M 1998 *Phys. Rev. A* **57** 1338
[19] Bae I H, Moon H S, Kim M K, Lee L and Kim J B 2008 *Appl. Opt.* **47** 4849
[20] Bae I H, Moon H S, Kim M K, Lee L and Kim J B 2010 *Opt. Express* **18** 1389
[21] Zhang J X, Zhou H T, Wang D W and Zhu S Y 2011 *Phys. Rev. A* **83** 053841
[22] Zhou H T, Wang D W, Wang D, Zhang J X and Zhu S Y 2011 *Phys. Rev. A* **84** 053835
[23] Affolderbach C, Knappe S, Wynands R, Taĭchenachev A V and Yudin V I 2002 *Phys. Rev. A* **65** 043810
[24] Andy W. Brown and Min Xiao 2005 *Opt. Lett.* **30** 699
[25] Zhou H T, Wang D, Guo M J, Gao J R and Zhang J X 2014 *Chin. Phys. B* **23** 093204
[26] Wang D W, Zhou H T, Guo M J, Zhang J X, Evers J and Zhu S Y 2013 *Phys. Rev. Lett.* **110** 093901
[27] Born M and Wolf E 1999 Principles of optics: electromagnetic theory of propagation, interference and diffraction of light (Cambridge: Cambridge University Press, UK), pp. 66–67
[28] Deutsch I H, Spreeuw R J C, Rolston S L and Phillips W D 1995 *Phys. Rev. A* **52** 1394
[29] Jackson J D 1975 Classical Electrodynamics, 2nd edn. (New York: Wiley), pp. 306–312